Turing's diffusive threshold in random reaction-diffusion systems

Pierre A. Haas*
Mathematical Institute, University of Oxford, Woodstock Road, Oxford OX2 6GG, United Kingdom

Raymond E. Goldstein†
Department of Applied Mathematics and Theoretical Physics, Centre for Mathematical Sciences, University of Cambridge, Wilberforce Road, Cambridge CB3 0WA, United Kingdom

(Dated: March 1, 2021)

Turing instabilities of reaction-diffusion systems can only arise if the diffusivities of the chemical species are sufficiently different. This threshold is unphysical in most systems with $N = 2$ diffusing species, forcing experimental realizations of the instability to rely on fluctuations or additional nondiffusing species. Here we ask whether this diffusive threshold lowers for $N > 2$ to allow "true" Turing instabilities. Inspired by May's analysis of the stability of random ecological communities, we analyze the probability distribution of the diffusive threshold in reaction-diffusion systems defined by random matrices describing linearized dynamics near a homogeneous fixed point. In the numerically tractable cases $N \leqslant 6$, we find that the diffusive threshold becomes more likely to be smaller and physical as N increases and that most of these many-species instabilities cannot be described by reduced models with fewer species.

In 1952, Turing described the pattern-forming instability that now bears his name [1]: diffusion can destabilize a fixed point of a system of reactions that is stable in well-mixed conditions. Nigh on threescore and ten years on, the contribution of Turing's mechanism to chemical and biological morphogenesis remains debated, not least because of the *diffusive threshold* inherent in the mechanism: chemical species in reaction systems are expected to have roughly equal diffusivities, yet Turing instabilities cannot arise at equal diffusivities [2, 3]. It remains an open problem to determine how much of a diffusivity difference is required for generic systems to undergo this instability, yet this diffusive threshold has been recognized at least since reduced models of the Belousov–Zhabotinsky reaction [4, 5] only produced Turing patterns at unphysically large diffusivity differences.

For this reason, the first experimental realizations of Turing instabilities [6–8] obviated the threshold by using gel reactors that greatly reduced the effective diffusivity of one species [9, 10]. (Analogously, biological membrane transport dynamics can increase the effective diffusivity difference [11].) Later work showed how binding to an immobile substrate, or more generally, a third, nondiffusing species, can allow Turing instabilities even if the $N = 2$ diffusing species have equal diffusivities [12–14]. Such nondiffusing species continue to permeate more recent work on the network topology of Turing systems [15, 16].

Moreover, Turing instabilities need not be deterministic: fluctuation-driven instabilities in reaction-diffusion systems have noise-amplifying properties that allow their pattern amplitude to be comparable to that of deterministic Turing patterns [17], with a lower diffusive threshold than the deterministic one [18–21]. A synthetic bacterial population with $N = 2$ species that exhibits patterns in agreement with such a stochastic Turing instability, but does not satisfy the conditions for a deterministic instability [22], was reported recently.

These experimental instabilities relying on fluctuations or the dynamics of additional nondiffusing species and the nonlinear instabilities arising from finite-amplitude perturbations [2] are not however instabilities in Turing's own image. Can such instabilities be realized instead in systems with $N > 2$ diffusing species? Equivalently, is the diffusive threshold lower in such systems? These questions have remained unanswered, perhaps because, in contrast to the textbook case $N = 2$ and the concomitant picture of an "inhibitor" out-diffusing an "activator" [23, 24], the complicated instability conditions for $N > 2$ [25] do not lend themselves to analytical progress.

Here, we analyze the diffusive threshold for Turing instabilities with $2 \leqslant N \leqslant 6$ diffusing species. Inspired by May's work on the stability of random ecological communities [26], we analyze *random Turing instabilities* by sampling random matrices that represent the linearized reaction dynamics of otherwise unspecified reaction-diffusion systems. A semianalytic approach shows that the diffusive threshold is more likely to be smaller and physical for $N = 3$ compared to $N = 2$, and that two of the three diffusivities are equal at the transition to instability. We extend these results to the remaining numerically tractable cases of reaction-diffusion systems with $4 \leqslant N \leqslant 6$ and two different diffusivities: their Turing instabilities are still more likely to have a smaller and physical diffusive threshold, but most of them cannot be described by reduced models with fewer species.

We begin with the simplest case, $N = 2$, in which species u, v obey

$$\dot{u} = f(u, v) + d_u \nabla^2 u, \qquad \dot{v} = g(u, v) + d_v \nabla^2 v. \tag{1}$$

The conditions for Turing instability in this system [24] only depend on the four entries of the Jacobian

$$\mathsf{J} = \begin{pmatrix} f_u & f_v \\ g_u & g_v \end{pmatrix}, \tag{2}$$

the partial derivatives of the reaction system at a fixed point (u_*, v_*) of the homogeneous system. This fixed point is stable to homogeneous perturbations iff $J \equiv \det \mathsf{J} > 0$ and $I_1 \equiv \operatorname{tr} \mathsf{J} < 0$. A stable fixed point of this kind is unstable to a Turing instability only if $p \equiv -f_u g_v > 0$ [24]. Defining the diffusion coefficient ratio $D_2 = \max\{d_u/d_v, d_v/d_u\} \geqslant 1$,

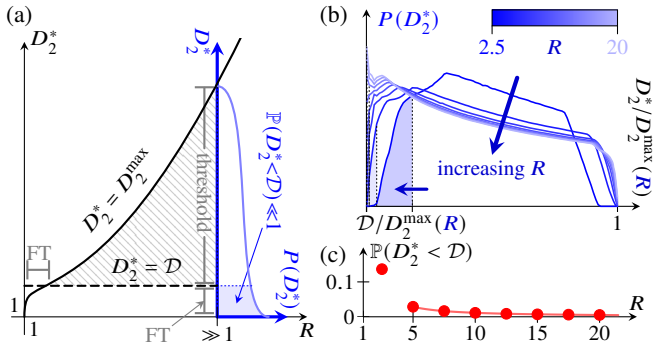

FIG. 1. Turing's diffusive threshold for $N = 2$. (a) Cartoon of the diffusive threshold and the fine-tuning (FT) problem for $R \approx 1$ and $R \gg 1$. The diffusivity difference required mathematically is unphysical in the hatched region $\mathcal{D} \leqslant D_2^* \leqslant D_2^{\max}$. (b) Distribution $P(D_2^*)$, supported on the (scaled) interval $[1, D_2^{\max}(R)]$, estimated for different R. (c) Plot of $\mathbb{P}(D_2^* < \mathcal{D})$ [shaded areas in panels (a) and (b)] against R, revealing the diffusive threshold. Markers: estimates from panel (b); solid line: exact result [27] for $R > \mathcal{D}$ [33].

a Turing instability occurs iff these conditions hold along with [27]

$$D_2 \geqslant D_2^* \equiv \left(\frac{\sqrt{J} + \sqrt{J+p}}{\min\{|f_u|, |g_v|\}} \right)^2 . \tag{3}$$

This diffusivity difference D_2^*, which is required mathematically for instability, is unphysical [Fig. 1(a)] if it exceeds the diffusivity difference $\mathcal{D} > 1$ of the physical system: $\mathcal{D} \approx 1$ for similarly sized molecules in solution, but, e.g., $\mathcal{D} \approx 20$ for the stochastic Turing instability observed in Ref. [22]. Hereinafter we take $\mathcal{D} = 5$ arbitrarily (but have checked that the value of $\mathcal{D}$ does not affect results qualitatively). To quantify D_2^*, we introduce the *range* R of kinetic parameters,

$$R \equiv \frac{\max\{|f_u|, |f_v|, |g_u|, |g_v|\}}{\min\{|f_u|, |f_v|, |g_u|, |g_v|\}} . \tag{4}$$

Equivalently, $f_u, f_v, g_u, g_v \in I \equiv [-R, -1] \cup [1, R]$ up to scaling, with one parameter equal to ± 1 and one equal to $\pm R$. One deduces [27] that

$$D_2^* \leqslant D_2^{\max}(R) \equiv \left(R + \sqrt{R^2 - 1} \right)^2 , \tag{5}$$

as shown in Fig. 1(a). Note that $D_2^{\max} \to 1$ as $R \to 1$; in this limit, there is no diffusive threshold: $R \approx 1$ is a particular instance of the converse *fine-tuning problem* for the reaction kinetics that allows Turing instabilities at nearly equal diffusivities more generally [3]. If $R \gg 1$, then $D_2^{\max} = O(R^2)$. This does not imply the existence of a threshold, for it does not preclude most systems with range R having $D_2^* \ll D_2^{\max}$. The existence of a diffusive threshold therefore relates to the distribution of D_2^* for systems with range R.

To understand this distribution, we draw inspiration from May's statistical analysis of the stability of ecological communities [26], which studies random Jacobians, corresponding to equilibria of otherwise unspecified population dynamics. By analogy, we study random Turing instabilities, sampling uniformly and independently random Jacobians corresponding to equilibria of otherwise unspecified reaction kinetics, and analyze the criteria for them to be Turing unstable. There is of course no more reason to expect the kinetic parameters to be independent or uniformly distributed than there is reason to expect the linearized population dynamics in May's analysis [26] to be independent or normally distributed. Yet, in the absence of experimental understanding of what the distributions of these parameters should be (in either context), the potential of the random matrix approach to reveal stability principles has been amply demonstrated in population dynamics [34–44].

We sample the kinetic parameters in Eq. (2) independently and uniformly from I, set one of them equal to ± 1 and one equal to $\pm R$, and thus estimate the probability distribution $P(D_2^*)$ for fixed R [Fig. 1(b)]. The threshold is quantified by the probability of a Turing instability being physical,

$$\mathbb{P}(D_2^* < \mathcal{D}) = \int_1^{\mathcal{D}} P(D_2^*)\, \mathrm{d}D_2^* . \tag{6}$$

Both from the estimates in Fig. 1(b) and by evaluating the integral in closed form [27], we find that $\mathbb{P}(D_2^* < \mathcal{D})$ is tiny [Fig. 1(c)], except if R is small, which is the fine-tuning problem again. In other words, the required diffusivity difference is very likely to be unphysical. This expresses Turing's diffusive threshold for $N = 2$.

To investigate how this threshold changes with N we consider next the $N = 3$ system

$$\dot{u} = f(u, v, w) + d_u \nabla^2 u, \tag{7a}$$

$$\dot{v} = g(u, v, w) + d_v \nabla^2 v, \tag{7b}$$

$$\dot{w} = h(u, v, w) + \nabla^2 w, \tag{7c}$$

where we have rescaled space to set $d_w = 1$. We introduce the matrix of diffusivities and the reaction Jacobian,

$$\mathsf{D} = \begin{pmatrix} d_u & 0 & 0 \\ 0 & d_v & 0 \\ 0 & 0 & 1 \end{pmatrix}, \qquad \mathsf{J} = \begin{pmatrix} f_u & f_v & f_w \\ g_u & g_v & g_w \\ h_u & h_v & h_w \end{pmatrix}, \tag{8}$$

in which the entries of J are again the partial derivatives evaluated at a fixed point (u_*, v_*, w_*) of the homogeneous system. This fixed point is unstable to a Turing instability if it is stable but, for some eigenvalue $-k^2 < 0$ of the Laplacian, $\bar{\mathsf{J}}(k^2) = \mathsf{J} - k^2\mathsf{D}$ is unstable [3], i.e. has an eigenvalue λ such that $\mathrm{Re}(\lambda) < 0$. More precisely, a Turing instability arises when a real eigenvalue of $\bar{\mathsf{J}}(k^2)$ crosses zero, i.e. when $\mathcal{J}(k^2) \equiv \det \bar{\mathsf{J}}(k^2) = 0$, and therefore arises first at a wavenumber $k = k_*$ with $\mathcal{J}(k_*^2) = \partial\mathcal{J}/\partial k^2(k_*^2) = 0$ [3]. Hence $\mathcal{J}$, a cubic polynomial in k^2, has a double root at $k^2 = k_*^2 > 0$, so its discriminant [29] vanishes. This discriminant, $\Delta(d_u, d_v)$, is a polynomial in d_u, d_v. We denote by $K(d_u, d_v)$ the double root of $\mathcal{J}$ corresponding to a point (d_u, d_v) on the curve $\Delta(d_u, d_v) = 0$.

Determining the diffusive threshold for Turing instability in Eqs. (7) thus requires solving the problem

$$\text{minimize } D_3(d_u, d_v) \quad \text{subject to} \begin{cases} \Delta(d_u, d_v) = 0, \\ K(d_u, d_v) > 0, \end{cases} \tag{9}$$

in which the diffusion coefficient ratio is

$$D_3(d_u, d_v) = \max\{d_u, 1/d_u, d_v, 1/d_v, d_u/d_v, d_v/d_u\}. \quad (10)$$

With the aim in mind of obtaining statistics for the minimal value D_3^*, direct numerical solution of this constrained optimization problem is obviously not a feasible approach. In the Supplemental Material [27], we therefore show how to reduce solving problem (9) to polynomial root finding. This semianalytic approach reveals a particular class of minima, attained at the vertices of the contours of $D_3(d_u, d_v)$ [Fig. 2(a)], i.e. at $d_u = 1$, $d_v = 1$, or $d_u = d_v$. In these cases, $\Delta(d_u, d_v) = 0$ is a (sextic) polynomial in the single variable d_v, d_u, or $d = d_u = d_v$, respectively. We call these minima "binary", since the corresponding systems have only two different diffusivities. We implement this approach numerically [27], and sample random systems similarly to the case $N = 2$, drawing the entries of J in Eq. (8) uniformly and independently at fixed range R.

Remarkably, all global minima we found numerically were binary [27]. This means that the minimizing systems come in two flavors: those with two "fast" diffusers and one "slow" diffuser, and those with one "fast" diffuser and two "slow" diffusers. Systems with a nondiffusing species are a limit of the former; this point will be discussed below. The latter arise in models of scale pattern formation in fish and lizards [45, 46], in which short-range pigments respectively activate and inhibit a long-range factor.

The distribution of D_3^*, shown for different values of R in Fig. 2(b), has a different shape from that of D_2^* [Figs. 1(a) and 2(b), inset]. While the support of the distribution of D_3^* does not appear to be bounded, Fig. 2(c) shows that $\mathbb{P}(D_3^* < \mathcal{D}) > \mathbb{P}(D_2^* < \mathcal{D})$. Hence the diffusivity difference is more likely to be physical for $N = 3$ than for $N = 2$: the diffusive threshold is lowered.

The proportion τ_N of random kinetic Jacobians that have a Turing instability (be it physical or unphysical) is smaller for $N = 3$ than for $N = 2$ [Fig. 2(d), inset]. This is not surprising, because a random Jacobian is less likely to correspond to a stable fixed point (which, we recall, is a necessary condition for Turing instability) for $N = 3$ than for $N = 2$, essentially because its entries have to satisfy more conditions for stability if $N = 3$. It is therefore striking that the threshold is reduced sufficiently for $N = 3$ compared to $N = 2$ for the proportion $\phi_N(\mathcal{D}) = \tau_N \mathbb{P}(D_N^* < \mathcal{D})$ of random Jacobians that have a physical Turing instability to be larger for $N = 3$ than for $N = 2$ [Fig. 2(d)], even though a Turing instability of any kind is more likely if $N = 2$.

To extend these results to $N > 3$ diffusing species, we consider the (linearized) reaction-diffusion system

$$\dot{\boldsymbol{u}} = \mathsf{J} \cdot \boldsymbol{u} + \mathsf{D} \cdot \nabla^2 \boldsymbol{u}, \quad (11)$$

where J is a random kinetic Jacobian, and D is a diagonal matrix of diffusivities. Even with our semianalytic approach, this cannot be analyzed for general D: not even for $N = 4$ were we able to obtain closed forms of the required polynomials. To make further progress, we therefore restrict to binary D in which the N diffusivities take two different values only, since we showed above that D_3^* is attained for such binary D. As in the case $N = 3$, this reduces the discriminant condition $\Delta(\mathsf{D}) = 0$ to polynomial equations in one variable that determine the minimum diffusivity difference D_N^* for Turing instability in these binary systems [27].

Figure 3(a) shows that the diffusive threshold lowers further for $4 \leqslant N \leqslant 6$ in these systems. At the same time, the fact that most stable random kinetic Jacobians undergo such a binary Turing instability [Fig. 3(b)] suggests that these provide a useful picture of the diffusive threshold. However, τ_N decreases further for $N \geqslant 4$ [Fig. 3(c), inset], and the widening of the

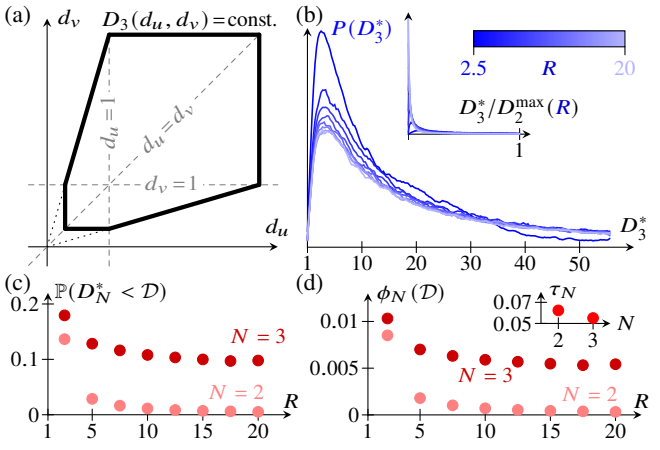

FIG. 2. Results for $N = 3$. (a) Contours of $D_3(d_u, d_v)$ in the positive (d_u, d_v) quadrant. (b) Smoothed distribution $P(D_3^*)$, estimated for different R. Inset: same plot, scaled to $[1, D_2^{\max}(R)]$ for comparison to $N = 2$ in Fig. 1(a). (c) $\mathbb{P}(D_N^* < \mathcal{D})$ against R for $N \in \{2, 3\}$: the diffusive threshold lowers for $N = 3$ compared to $N = 2$. (d) Proportion $\phi_N(\mathcal{D})$ of random Jacobians that have a physical Turing instability, plotted against R, for $N \in \{2, 3\}$. Inset: proportion τ_N of random Jacobians that have a (physical or unphysical) Turing instability, averaged over R, for $N \in \{2, 3\}$ [33].

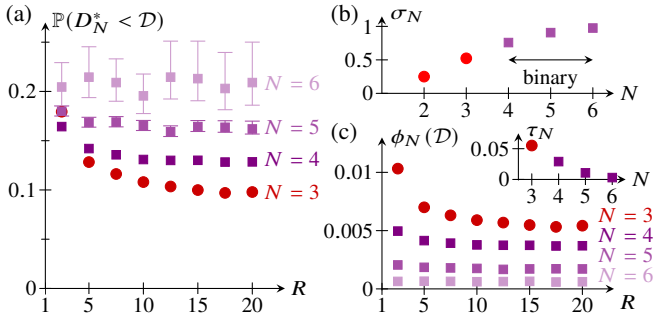

FIG. 3. Results for "binary" systems with $4 \leqslant N \leqslant 6$. (a) $\mathbb{P}(D_N^* < \mathcal{D})$ against R for $3 \leqslant N \leqslant 6$, revealing further lowering of the diffusive threshold compared to the case $N = 3$. (b) Proportion σ_N of random stable kinetic Jacobian that have a (binary, if $N > 3$) Turing instability, averaged over R, and plotted against N. (c) Proportion $\phi_N(\mathcal{D})$ of random Jacobians that have a physical Turing instability plotted against R, for $3 \leqslant N \leqslant 6$. Inset: proportion τ_N of random Jacobians that have a (physical or unphysical) Turing instability, averaged over R, for $3 \leqslant N \leqslant 6$ [33].

bottleneck is not sufficient to prevent $\phi_N(\mathcal{D})$ from decreasing for $N \geqslant 4$. Nonetheless, since both $\mathbb{P}(D_N^* < \mathcal{D})$ and the proportion σ_N of stable random Jacobians that are Turing unstable increase [Figs. 3(a) and 3(b)], so does the proportion of stable random Jacobians that have a physical Turing instability.

How then to realize "true" Turing instabilities experimentally? Our analysis shows that the diffusive threshold of a Turing instability is more likely to be physical the more species there are, but how to find an experimental Turing instability in the first place? Turing instabilities remain rare in random reaction systems even as the number of species is increased, but the above shows that this rareness mainly results from the rareness of stable equilibria in such systems. The proverbial search for the needle in a haystack can therefore be avoided by exploring biochemical systems that admit a stable equilibrium, and evolving them towards a "true" Turing instability.

This analysis does not however reveal whether these instabilities lead to patterns that are observable at the physical scale of the system. Analysis of the wavenumber at which the linear instability first arises [27] suggests that we can extend our conclusions: Turing instabilities with more species are more likely to have physical diffusivity differences and to be observable. However, our statistical, linearized analysis cannot fully answer this question of observability, because it fundamentally depends on the system through details of the nonlinearities of its reaction kinetics, which set the precise nature and scale of the Turing patterns that develop beyond onset of the instability; this is why we have relegated this discussion to the Supplemental Material [27].

The different species in the systems with $3 \leqslant N \leqslant 6$ analyzed above separate into "fast" and "slow" diffusers. The diffusion of these "slow" species is often ignored in the analysis of systems of many chemical reactions [30], such as the full Belousov–Zhabotinsky reaction [47]. Corresponding reduced models are obtained by substituting the steady-state kinetics of the "slow" species into the remaining equations, thereby eliminating them from the system [30]. The conditions for Turing instability in these reduced models are (almost) equivalent to those for the full model with nondiffusing "slow" species [30]. However, the diffusion of the "slow" species cannot in general be ignored: up to reordering species and rescaling space,

$$\mathsf{D} = \left(\begin{array}{c|c} \mathsf{I} & \mathsf{0} \\ \hline \mathsf{0} & d\mathsf{I} \end{array}\right), \qquad \mathsf{J} = \left(\begin{array}{c|c} \mathsf{J}_{11} & \mathsf{J}_{12} \\ \hline \mathsf{J}_{21} & \mathsf{J}_{22} \end{array}\right), \tag{12}$$

where $d < 1$ is the common diffusivity of the slow diffusers. Results of Ref. [30] imply that there is a Turing instability with nondiffusing "slow" species, i.e. with $d = 0$, only if $\mathsf{J}_{11} - \mathsf{J}_{12}\mathsf{J}_{22}^{-1}\mathsf{J}_{21}$ has a positive (real) eigenvalue [27]. Although the proportion of Turing unstable systems that have $n \geqslant 2$ fast diffusers (and hence could *a priori* still undergo a Turing instability with $d = 0$) is large [Fig. 4(a)], the proportion of systems that do undergo such an instability is small, even if we restrict to those systems with physical diffusivity differences [Fig. 4(b)]. Hence most of these Turing instabilities with $N > 2$ species require all species to diffuse.

These many-species Turing instabilities, although binary, are thus more general than the instabilities of systems with

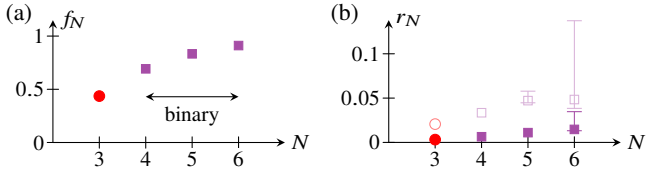

FIG. 4. "Slow" diffusers in binary Turing instabilities with $3 \leqslant N \leqslant 6$. (a) Proportion f_N of Turing unstable systems with $n \geqslant 2$ "fast" diffusers plotted against N, averaged over R. (b) Proportion r_N of systems that remain Turing unstable at $d = 0$, plotted against N, averaged over R. Closed markers: all Turing systems; open markers: physical Turing systems with $D_N^* < \mathcal{D}$ [33].

nondiffusing species realized experimentally in gel reactors [6–8] and analyzed theoretically in Ref. [30]. In particular, this shows that reduced models give but an incomplete picture of Turing instabilities. Together with our main result, that the diffusive threshold lowers as N increases, this implies that the failure of a reduced model to produce a physical Turing instability cannot be taken as an indication that a Turing instability cannot exist in the full system that the reduced model seeks to describe.

In this Letter, we have analyzed random Turing instabilities to show how the diffusive threshold that has hampered experimental efforts to generate "true" Turing instabilities in systems of $N = 2$ diffusing species lowers for systems with $N \geqslant 3$, most of whose instabilities cannot be described by reduced models with fewer species. All of this does not, however, explain the existence of a "large" threshold in the first place: even though Turing instabilities at equal diffusivities are impossible [2, 3], this does not mean that the threshold needs to be "large". In this context, we prove an asymptotic result in the Supplemental Material [27]: for a Jacobian J to allow a Turing instability at almost equal diffusivities $\mathsf{D} \approx \mathsf{I}$, J must be even closer to a singular matrix J_0, i.e. $\mathsf{J} - \mathsf{J}_0 \ll \mathsf{D} - \mathsf{I}$. In this sense, the threshold $\mathsf{D} - \mathsf{I}$ is asymptotically "large". Understanding how a large threshold arises more generally outside this asymptotic regime and lowers as N increases remains an open problem, as do extending the present analysis to include the nonlocal interactions [48, 49] that arise for example in vegetation patterns [50] and extending previous work [16, 51] on the robustness of Turing patterns to $N \geqslant 3$. The latter in particular may help to identify those chemical or biological pattern forming systems with $N \geqslant 3$ in which the "true" Turing instabilities discussed here can be realized experimentally.

We thank N. Goldenfeld, A. Krause, and P. K. Maini for discussions. This work was supported in part by a Nevile Research Fellowship from Magdalene College, Cambridge, and a Hooke Research Fellowship (P.A.H.), Established Career Fellowship EP/M017982/1 from the Engineering and Physical Sciences Research Council and Grant 7523 from the Marine Microbiology Initiative of the Gordon and Betty Moore Foundation (R.E.G.).

* haas@pks.mpg.de; current address: Max Planck Institute for the Physics of Complex Systems, Nöthnitzer Straße 38, 01187 Dresden, Germany

† r.e.goldstein@damtp.cam.ac.uk

[1] A. M. Turing, The chemical basis of morphogenesis, Phil. Trans. R. Soc. B **237**, 37 (1952).

[2] J. A. Vastano, J. E. Pearson, W. Horsthemke, and H. L. Swinney, Chemical pattern formation with equal diffusion coefficients, Phys. Lett. A **124**, 320 (1987).

[3] J. E. Pearson and W. Horsthemke, Turing instabilities with nearly equal diffusion coefficients, J. Chem. Phys. **90**, 1588 (1989).

[4] P. K. Becker and R. J. Field, Stationary concentration patterns in the oregonator model of the Belousov–Zhabotinskii reaction, J. Phys. Chem. **89**, 118 (1985).

[5] A. B. Rovinskii, Turing bifurcation and stationary patterns in the ferroin-catalyzed Belousov–Zhabotinskii reaction, J. Phys. Chem. **91**, 4606 (1987).

[6] V. Castets, E. Dulos, J. Boissonade, and P. De Kepper, Experimental evidence of a sustained standing Turing-type nonequilibrium chemical pattern, Phys. Rev. Lett. **64**, 2953 (1990).

[7] P. De Kepper, V. Castets, E. Dulos, and J. Boissonade, Turing-type chemical patterns in the chlorite-iodide-malonic acid reaction, Physica D **49**, 161 (1991).

[8] Q. Ouyang and H. L. Swinney, Transition from a uniform state to hexagonal and striped Turing patterns, Nature (London) **352**, 610 (1991).

[9] I. Lengyel and I. R. Epstein, Modeling of Turing structures in the chloride-iodid-malonic acid-starch reaction system, Science **251**, 650 (1991).

[10] E. Dulos, J. Boissonade, J. J. Perraud, B. Rudovics, and P. De Kepper, Chemical morphogenesis: Turing patterns in an experimental chemical system, Acta Biother. **44**, 249 (1996).

[11] P. Recho, A. Hallou, and E. Hannezo, Theory of mechanochemical patterning in biphasic biological tissues, Proc. Natl. Acad. Sci. USA **116**, 5344 (2019).

[12] I. Lengyel and I. R. Epstein, A chemical approach to designing Turing patterns in reaction-diffusion systems, Proc. Natl. Acad. Sci. USA **89**, 3977 (1992).

[13] J. E. Pearson, Pattern formation in a $(2 + 1)$-species activator-inhibitor-immobilizer system, Physica A **188**, 178 (1992).

[14] K. Korvasová, E. A. Gaffney, P. K. Maini, M. A. Ferreira, and V. Klika, Investigating the Turing conditions for diffusion-driven instability in the presence of a binding immobile substrate, J. Theor. Biol. **367**, 286 (2015).

[15] L. Marcon, X. Diego, J. Sharpe, and P. Müller, High-throughput mathematical analysis identifies Turing networks for patterning with equally diffusing signals, eLife **5**, e14022 (2016).

[16] X. Diego, L. Marcon, P. Müller, and J. Sharpe, Key features of Turing systems are determined purely by network topology, Phys. Rev. X **8**, 021071 (2018).

[17] T. Biancalani, F. Jafarpour, and N. Goldenfeld, Giant amplification of noise in fluctuation-induced pattern formation, Phys. Rev. Lett. **118**, 018101 (2017).

[18] T. Butler and N. Goldenfeld, Robust ecological pattern formation induced by demographic noise, Phys. Rev. E **80**, 030902(R) (2009).

[19] T. Biancalani, D. Fanelli, and F. Di Patti, Stochastic Turing patterns in the Brusselator model, Phys. Rev. E **81**, 046215 (2010).

[20] T. Butler and N. Goldenfeld, Fluctuation-driven Turing patterns, Phys. Rev. E **84**, 011112 (2011).

[21] F. Di Patti, L. Lavacchi, R. Arbel-Goren, L. Schein-Lubomirsky, D. Fanelli, and J. Stavans, Robust stochastic turing patterns in the development of a one-dimensional cyanobacterial organism, PLoS Biol. **16**, e2004877 (2018).

[22] D. Karig, K. M. Martini, T. Lu, N. A. DeLateur, N. Goldenfeld, and R. Weiss, Stochastic Turing patterns in a synthetic bacterial population, Proc. Natl. Acad. Sci. USA **115**, 6572 (2018).

[23] A. J. Koch and H. Meinhardt, Biological pattern formation: from basic mechanisms to complex structures, Rev. Mod. Phys. **66**, 1481 (1994).

[24] J. D. Murray, in *Mathematical Biology* (Springer, Berlin, Germany, 2002) Vol. I, Appendix B.1, pp. 507–509 and Vol. II, Chap. 2, pp. 71–140, 3rd ed.

[25] R. A. Satnoianu, M. Menzinger, and P. K. Maini, Turing instabilities in general systems, J. Math. Biol. **41**, 493 (2000).

[26] R. M. May, Will a large complex ecosystem be stable?, Nature (London) **238**, 413 (1972).

[27] See Supplemental Material at [url to be inserted], which includes Refs. [3, 24, 28–32], for details of calculations for $N = 2$, the derivation of the semianalytic approach for $N > 2$ and a discussion of its numerical implementation, statistics of the wavenumber of Turing instabilities, a discussion of "slow" species, the proof of an asymptotic result, and for `python3` code.

[28] F. Johansson, *`mpmath`: a `python` library for arbitrary-precision floating-point arithmetic* (version 1.1.0, 2018).

[29] C.-K. Yap, in *Fundamental Problems in Algorithmic Algebra* (Oxford University Press, Oxford, England, 2000) Chap. 6 and Chap. 7, pp. 141–218.

[30] S. Smith and N. Dalchau, Model reduction enables Turing instability analysis of large reaction–diffusion models, J. R. Soc. Interface **15**, 20170805 (2018).

[31] E. J. Hinch, in *Perturbation Methods* (Cambridge University Press, Cambridge, UK, 1991) Chap. 1.6, pp. 15–18.

[32] V. B. Lidskii, Perturbation theory of non-conjugate operators, USSR Comput. Math. Math. Phys. **6**, 73 (1966).

[33] All results shown are for $\mathcal{D} = 5$. The asymmetric error bars in Figs. 3 and 4 show 95% confidence intervals larger than the plot markers, corrected for systems for which the numerics failed.

[34] S. Allesina and S. Tang, Stability criteria for complex ecosystems, Nature (London) **483**, 205 (2012).

[35] A. Mougi and M. Kondoh, Diversity of interaction types and ecological community stability, Science **337**, 349 (2012).

[36] K. Z. Coyte, J. Schluter, and K. R. Foster, The ecology of the microbiome: Networks, competition, and stability, Science **350**, 663 (2015).

[37] J. Grilli, T. Rogers, and S. Allesina, Modularity and stability in ecological communities, Nat. Commun. **7**, 12031 (2016).

[38] T. Gibbs, J. Grilli, T. Rogers, and S. Allesina, Effect of population abundances on the stability of large random ecosystems, Phys. Rev. E **98**, 022410 (2018).

[39] C. A. Serván, J. A. Capitán, J. Grilli, K. E. Morrison, and S. Allesina, Coexistence of many species in random ecosystems, Nat. Ecol. Evol. **2**, 1237 (2018).

[40] S. Butler and J. P. O'Dwyer, Stability criteria for complex microbial communities, Nat. Commun. **9**, 2970 (2018).

[41] L. Stone, The feasibility and stability of large complex biological networks: a random matrix approach, Sci. Rep. **8**, 8246 (2018).

[42] D. S. Maynard, C. A. Serván, J. A. Capitán, and S. Allesina, Phenotypic variability promotes diversity and stability in competitive communities, Ecol. Lett. **22**, 1776 (2019).

[43] P. A. Haas, N. M. Oliveira, and R. E. Goldstein, Subpopulations and stability in microbial communities, Phys. Rev. Research **2**, 022036(R) (2020).

[44] J. W. Barron and T. Galla, Dispersal-induced instability in complex ecosystems, Nat. Commun. **11**, 6032 (2020).

[45] A. Nakamasu, G. Takahashi, A. Kanbe, and S. Kondo, Interactions between zebrafish pigment cells responsible for the generation of Turing patterns, Proc. Natl. Acad. Sci. USA **106**, 8429 (2009).

[46] L. Manukyan, S. A. Montandon, A. Fofonjka, S. Smirnov, and M. C. Milinkovitch, A living mesoscopic cellular automaton made of skin scales, Nature (London) **544**, 173 (2017).

[47] L. Györgi, T. Turányi, and R. J. Field, Mechanistic details of the

oscillator Belousov–Zhabotinskii reaction, J. Phys. Chem. **94**, 7162 (1990).

[48] T. Ohta, M. Mimura, and R. Kobayashi, Higher-dimensional localized patterns in excitable media, Physica D **34**, 115 (1989).

[49] R. E. Goldstein, D. J. Muraki, and D. M. Petrich, Interface proliferation and the growth of labyrinths in a reaction-diffusion system, Phys. Rev. E **53**, 3933 (1996).

[50] E. Meron, Vegetation pattern formation: The mechanisms behind the forms, Physics Today **72**, 30 (2019).

[51] N. S. Scholes, D. Schnoerr, M. Isalan, and M. P. H. Stumpf, A comprehensive network atlas reveals that Turing patterns are common but not robust, Cell Systems **9**, 243 (2019).

Turing's diffusive threshold in random reaction-diffusion systems
— Supplemental Material —

Pierre A. Haas
Mathematical Institute, University of Oxford, Woodstock Road, Oxford OX2 6GG, United Kingdom

Raymond E. Goldstein
Department of Applied Mathematics and Theoretical Physics, Centre for Mathematical Sciences, University of Cambridge, Wilberforce Road, Cambridge CB3 0WA, United Kingdom

This Supplemental Material is divided into five sections, which provide (i) details of calculations for $N = 2$, (ii) the derivation of the semianalytic approach for $N = 3$ and a discussion of its numerical implementation, (iii) an analysis of the statistics of the wavenumber at which a Turing instability first arises, (iv) a discussion of Turing instabilities with nondiffusing "slow" species, and (v) a proof of the asymptotic result claimed in the conclusion of our Letter.

I. DETAILS OF CALCULATIONS FOR $N = 2$

A. Derivation of Eq. (3)

The form of the condition for Turing instability in Eq. (3) follows from that in Eq. (2.26) on page 85 of Vol. II of Ref. [S1] which, in our notation, reads

$$f_u + dg_v \geqslant 2\sqrt{dJ}, \tag{S1}$$

a quadratic in $d = d_u/d_v$. Hence

$$\sqrt{d} \gtrless \sqrt{d_*} \equiv \frac{\sqrt{J} \pm \sqrt{J - f_u g_v}}{g_v} \quad \text{if } g_v \gtrless 0. \tag{S2}$$

We notice that Eq. (S1) requires $f_u + dg_v \geqslant 0$. Since $I_1 < 0$, this implies that $d \gtrless 1$ if $g_v \gtrless 0$. Hence $D_2^* = d_*$ if $g_v > 0$, but $D_2^* = 1/d_*$ if $g_v < 0$. Now, if $g_v \gtrless 0$, then $|f_u| \gtrless |g_v|$ because $I_1 < 0$ and $p > 0$. Equation (3) then follows, since

$$\frac{g_v}{\sqrt{J} - \sqrt{J+p}} = \frac{\sqrt{J} + \sqrt{J+p}}{f_u}. \tag{S3}$$

B. Derivation of Eq. (5)

Equation (3) shows that D_2^* is continuous on I^4, so attains its maximum value on that domain. Since $p > 0$ and $J > 0$, $q \equiv -f_v g_u > 0$, so that $J + p = q$. Now D_2^* only depends on f_v, g_u through q, and, by direct computation from Eq. (3),

$$\frac{\partial D_2^*}{\partial q} = \frac{D_2^*}{\sqrt{J(J+p)}} > 0. \tag{S4}$$

Hence D_2^* increases with q, so $(f_v, g_u) = \pm(R, -R)$ at the maximum.

Now assume that $|f_u| \geqslant |g_v|$. Since $I_1 < 0$ and $|f_u| \geqslant |g_v|$, it follows that $f_u < 0$ and $g_v > 0$. Then

$$\frac{\partial D_2^*}{\partial f_u} = \frac{\sqrt{J} + \sqrt{q}}{g_v\sqrt{J}} > 0, \quad \frac{\partial D_2^*}{\partial g_v} = -\frac{\left(\sqrt{J} + \sqrt{q}\right)^3}{g_v^3\sqrt{J}} < 0, \tag{S5}$$

and so $(f_u, g_v) = (1, -1)$ at the maximum. If $|f_u| \leqslant |g_v|$, we similarly find that $(f_u, g_v) = (-1, 1)$ at the maximum. Substituting these values into Eq. (3) yields Eq. (5).

C. Calculation of $\mathbb{P}(D_2^* < \mathcal{D})$ for $\mathcal{D} \leqslant R$

There are 48 ways of assigning values ± 1 and $\pm R$ to two of the entries f_u, f_v, g_u, g_v of J. Integrating the conditions for Turing instability of the remaining entries in each of these cases using Mathematica (Wolfram, Inc.) gives the area of parameter space in which a Turing instability arises,

$$\iiiint_{I^4} \mathbb{1}\begin{pmatrix} J > 0,\ I_1 < 0 \\ p > 0 \\ \max|\mathsf{J}| = R \\ \min|\mathsf{J}| = 1 \end{pmatrix} \mathrm{d}\mathsf{J} = 12(R-1)^2, \tag{S6}$$

where we use the shorthand $\mathrm{d}\mathsf{J} = \mathrm{d}f_u\,\mathrm{d}f_v\,\mathrm{d}g_u\,\mathrm{d}g_v$. To analyze the condition $D_2^* < R$, we note that the expression for D_2^* in Eq. (3) shows that we may swap f_u, g_v and f_v, g_u. Hence the 48 cases reduce to 4 cases (corresponding to the entries ± 1 or $\pm R$ being on the the same or on different diagonals):

(1) $|f_u| = R, |g_v| = 1$; (2) $|f_v| = R, |g_u| = 1$;
(3) $|f_u| = R, |f_v| = 1$; (4) $|f_u| = 1, |f_v| = R$.

Moreover, since $q > 0$, we may take $f_v > 0$ and $g_u < 0$ without loss of generality. We now discuss these cases separately.

(1) $I_1 < 0$ implies $f_u = -R$, $g_v = 1$, and so

$$D_2^* = \left(\sqrt{q} + \sqrt{q-R}\right)^2 \geqslant R. \tag{S7}$$

(2) $f_u g_v = -R$ since $q > 0$, so $J = f_u g_v + R$.

(3) $f_u = -R$ because $I_1 < 0$. Now $p, q > 0$, and so $0 < J = -R|g_v| - |g_u| < 0$. This is a contradiction.

(4) $f_u = 1$ as $I_1 < 0$. Since $g_v \leqslant -1$, it follows that

$$D_2^* = \left(\sqrt{-g_u R} + \sqrt{-g_u R - g_v}\right)^2 \geqslant R. \tag{S8}$$

In this way, $D_2^* < R$ quantifies the diffusive threshold in a natural way. In particular, $D_2^* < R$ is only possible in case (2). Since $J > 0$, we require $f_u g_v + R > 0$ in that case. Now $I_1 < 0$ and $p > 0$, so $1 < f_u < -R/g_v$ or $1 < g_v < -R/f_u$ depending on $f_u > 0, g_v < 0$ or $f_u < 0, g_v > 0$. Assume without loss

of generality that $|f_u| \geqslant |g_v|$. Then $f_u < 0$, $g_v > 0$ as $I_1 < 0$. Moreover, using Eq. (3), $D_2^* = R$ if and only if $g_v = 2 + f_u/R$. From Eqs. (S5), D_2^* decreases as g_v increases. Hence

$$D_2^* < R \iff 2 + f_u/R < g_v \leqslant -R/f_u \text{ and } f_u + g_v < 0, \tag{S9}$$

using the conditions derived previously. Note that $-R/f_u < R$ and $2 + f_u/R > 1$ for $-R < f_u < -1$. If $|f_u| < |g_v|$, f_u, g_v are swapped in these conditions. Moreover, since $q > 0$, case (2) corresponds to 4 of the 48 cases. Hence we obtain, again using MATHEMATICA,

$$\iiiint_{I^4} \mathbb{1}\begin{pmatrix} J > 0,\ I_1 < 0 \\ p > 0,\ D_2^* < R \\ \max|\mathsf{J}| = R \\ \min|\mathsf{J}| = 1 \end{pmatrix} \mathrm{d}\mathsf{J} = 4\left(\frac{2R(1-R)}{1+R} + R\log R\right). \tag{S10}$$

Equations (S6) and (S10) imply

$$\mathbb{P}\left(D_2^* < R\right) = \frac{R\left[(R+1)\log R - 2(R-1)\right]}{3(R-1)^2(R+1)}. \tag{S11}$$

In particular, $\mathbb{P}\left(D_2^* < R\right) = O(\log R/R) \ll 1$ for $R \gg 1$. This statement expresses the existence of the diffusive bottleneck mathematically.

From a more physical point of view, as discussed in our Letter, it is more natural to consider the probability $\mathbb{P}\left(D_2^* < \mathcal{D}\right)$, for some constant $\mathcal{D} > 1$. Since "small" values $R \leqslant \mathcal{D}$ require fine-tuning of the reaction kinetics, we restrict to $\mathcal{D} \leqslant R$, so that $D_2^* < \mathcal{D}$ is only possible in case (2) above. We consider again the case $g_v > 0$, $f_u < 0$. Similarly to the derivation of conditions (S9), we find

$$D_2^* < \mathcal{D} \iff g_v > \sqrt{\frac{R}{\mathcal{D}}},\quad -\frac{R}{g_v} \leqslant f_u < \mathcal{D}g_v - 2\sqrt{\mathcal{D}R} \text{ and } f_u + g_v < 0. \tag{S12}$$

In particular,

$$-\frac{R}{g_v} = \max\left\{-R, -\frac{R}{g_v}\right\} \leqslant f_u < \min\left\{-1, -g_v, \mathcal{D}g_v - 2\sqrt{\mathcal{D}R}\right\}, \tag{S13a}$$

in which, since $g_v \geqslant 1$,

$$\min\left\{-1, -g_v, \mathcal{D}g_v - 2\sqrt{\mathcal{D}R}\right\} = \begin{cases} -g_v & \text{if } g_v > \dfrac{2\sqrt{\mathcal{D}R}}{\mathcal{D}+1}; \\ \mathcal{D}g_v - 2\sqrt{\mathcal{D}R} & \text{otherwise.} \end{cases} \tag{S13b}$$

We notice that $\sqrt{R} > 2\sqrt{\mathcal{D}R}/(\mathcal{D}+1) > \sqrt{R/\mathcal{D}}$ since $\mathcal{D} > 1$, and also that $\mathcal{D}g_v - 2\sqrt{\mathcal{D}R} > -R/g_v \iff \left(\sqrt{\mathcal{D}}g_v - \sqrt{R}\right)^2 > 0$, but $-g_v/-R/g_v \iff g_v < \sqrt{R}$. The area of parameter space described by conditions (S12) is therefore

$$\int_{\frac{2\sqrt{\mathcal{D}R}}{\mathcal{D}+1}}^{\sqrt{R}} \left(\int_{-\frac{R}{g_v}}^{-g_v} \mathrm{d}f_u\right)\mathrm{d}g_v + \int_{\sqrt{\frac{R}{\mathcal{D}}}}^{\frac{2\sqrt{\mathcal{D}R}}{\mathcal{D}+1}} \left(\int_{-\frac{R}{g_v}}^{\mathcal{D}g_v - 2\sqrt{\mathcal{D}R}} \mathrm{d}f_u\right)\mathrm{d}g_v = \frac{R}{2}\log\mathcal{D} - \frac{\mathcal{D}-1}{\mathcal{D}+1}R. \tag{S14a}$$

Hence [S2]

$$\iiiint_{I^4} \mathbb{1}\begin{pmatrix} J > 0,\ I_1 < 0 \\ p > 0,\ D_2^* < \mathcal{D} \\ \max|\mathsf{J}| = R \\ \min|\mathsf{J}| = 1 \end{pmatrix} \mathrm{d}\mathsf{J} = 4\left[2\left(\frac{R}{2}\log\mathcal{D} - \frac{\mathcal{D}-1}{\mathcal{D}+1}R\right)\right], \tag{S14b}$$

for $R > \mathcal{D}$, and, as above, we conclude that, for $R > \mathcal{D}$,

$$\mathbb{P}\left(D_2^* < \mathcal{D}\right) = \frac{R}{3(R-1)^2}\left[\log\mathcal{D} - \frac{2(\mathcal{D}-1)}{\mathcal{D}+1}\right]. \tag{S15}$$

D. Nondimensionalization

We close by remarking on the (absence of) nondimensionalization of the reaction system. Indeed, up to rescaling time, one among f_u, f_v, g_u, g_v can be set equal to ± 1. Moreover, one more parameter can be set equal to ± 1 by rescaling u, v differently. However, if we made those choices, we could no longer sample from a fixed interval.

II. SEMIANALYTIC METHOD FOR $N = 3$

A. Derivation of the semianalytic method

1. *Preliminary observations*

Before deriving the semianalytic method, we need to make two preliminary observations.

First, the necessary and sufficient (Routh–Hurwitz) conditions for the homogeneous system to be stable include $I_1 \equiv \operatorname{tr}\mathsf{J} < 0$ and $J \equiv \det\mathsf{J} < 0$ [S1]. By definition, $\bar{\mathsf{J}}(k_*^2)$ has one zero eigenvalue. The other two eigenvalues are either real or two complex conjugates λ, λ^*. In the second case, they are both stable (i.e. have negative real parts) since

$$2\operatorname{Re}(\lambda) = 0 + \lambda + \lambda^* = \operatorname{tr}\bar{\mathsf{J}}(k_*^2) = I_1 - k_*^2\operatorname{tr}\mathsf{D} < I_1 < 0. \tag{S16}$$

Hence Eqs. (7) are not unstable to an oscillatory (Turing–Hopf) instability at (d_u^*, d_v^*), so, by minimality of (d_u^*, d_v^*), the system destabilizes to a Turing instability there.

Moreover, since $\mathcal{J}$, viewed as a polynomial in k_*^2, has leading coefficient $-d_u d_v$ and constant term $\mathcal{J}(0) = J < 0$, the double root $K(d_u, d_v)$ varies continuously with d_u, d_v and cannot change sign on a branch of $\Delta(d_u, d_v) = 0$ in the positive (d_u, d_v) quadrant.

2. *Reduction of problem (9) to polynomial equations*

The discriminant of $\mathcal{J}$, viewed as a polynomial in the two variables d_u, d_v, is

$$\Delta(d_u, d_v) = \sum_{m=0}^{4}\sum_{n=0}^{4}\delta_{mn}d_u^m d_v^n, \tag{S17}$$

where $\delta_{00} = \delta_{10} = \delta_{01} = \delta_{34} = \delta_{43} = \delta_{44} = 0$ and (complicated) expressions for the 19 non-zero coefficients can be found in terms of the entries of J using MATHEMATICA (Wolfram, Inc.).

The second remark above implies that, at a local minimum of $D_3(d_u, d_v)$ on $\Delta(d_u, d_v) = 0$, one of the following occurs:

(i) $\Delta(d_u, d_v) = 0$ is tangent to a contour of $D_3(d_u, d_v)$;

(ii) $\Delta(d_u, d_v)$ intersects a vertex of a contour of $D_3(d_u, d_v)$;

(iii) $\Delta(d_u, d_v)$ is singular.

The contours of $D_3(d_u, d_v)$ are drawn in Fig. 2(a) of our Letter and show that tangency to a contour in case (i) requires

$$\mathrm{d}d_u = 0 \quad \text{or} \quad \mathrm{d}d_v = 0 \quad \text{or} \quad \mathrm{d}d_v/\mathrm{d}d_u = d_v/d_u. \tag{S18}$$

Since $\Delta(d_u, d_v) = 0$, the chain rule reads

$$0 = \mathrm{d}\Delta = \frac{\partial\Delta}{\partial d_u}\,\mathrm{d}d_u + \frac{\partial\Delta}{\partial d_v}\,\mathrm{d}d_v. \tag{S19}$$

Hence there are two subcases:

(a) $\dfrac{\partial\Delta}{\partial d_v} = 0$ or $\dfrac{\partial\Delta}{\partial d_u} = 0$;

(b) $d_u \dfrac{\partial\Delta}{\partial d_u} + d_v \dfrac{\partial\Delta}{\partial d_v} = 0$.

In subcase (a), Δ viewed as a polynomial in d_v or d_u has a double root, and so its discriminant [S3] must vanish. On removing zero roots, this discriminant of a discriminant is found to be a polynomial of degree 20 in d_u or d_v, respectively; complicated expressions for its coefficients in terms of the non-zero coefficients δ_{mn} in Eq. (S17) are obtained using MATHEMATICA. Similarly, in subcase (b), the resultant [S3] of Δ and $d_u\partial\Delta/\partial d_u + d_v\partial\Delta/\partial d_v$, viewed as polynomials in d_u or d_v must vanish. This resultant is another polynomial of degree 20 in d_v or d_u.

Next, in case (ii), $d_u = 1$ or $d_v = 1$ or $d_u = d_v$ [Fig. 2(a)], which reduces Δ to three different polynomials in the single variable d_v, d_u, or $d = d_u = d_v$, respectively. These polynomials have degree 6.

Finally, in case (iii), we note that, at a singular point, $\Delta = \partial\Delta/\partial d_u = \partial\Delta/\partial d_v = 0$, and so we are back in case (i), subcase (a).

Thus, we have reduced finding candidates for local minima in (9) to solving polynomial equations: this defines our semianalytic approach. The global minimum is found among those local minima with $K(d_u, d_v) > 0$; in case (i), the roots only correspond to local minima if additionally $d_u, d_v > 1$ or $d_u, d_v < 1$ in subcase (a) and $d_u < 1 < d_v$ or $d_v < 1 < d_u$ in subcase (b) [Fig. 2(a)].

3. *Extension to binary systems with $N > 3$*

For binary systems, the diagonal entries of D take two different values, d_1, d_2 only. Up to rescaling space, $d_1 = 1$ and $d_2 = d$, which turns the condition $\Delta(\mathsf{D}) = 0$ into $2^{N-1} - 1$ different polynomial equations in the single variable d, corresponding to the different combinatorial ways of assigning diffusivities d_1, d_2 to the N species (in such a way that not all species have the same diffusivity). Determining the minimum value D_N^* of $D_N = \max\{d, 1/d\}$ for these binary systems is thus reduced, again, to solving polynomial equations.

The argument we used above to show that coexistence of Turing and Turing–Hopf instabilities is not possible for $N = 3$ does not, however, carry over to $N > 3$. Numerically, it turns out, however, that systems in which Turing and Turing–Hopf instabilities coexist are rare. We therefore treat these systems in the same way as we treat systems for which the numerics fail (as discussed below).

B. Numerical implementation

Implementing the semi-analytical approach for $N = 3$ and its extension to binary systems with $4 \leqslant N \leqslant 6$ numerically takes some care as the coefficients of the polynomials that arise can range over many orders of magnitude. Our `python3` implementation therefore uses the `mpmath` library for variable precision arithmetic [S4].

To determine the positive real roots of the polynomials that arise in the semi-analytical approach, we complement the Durand–Kerner complex root finding implemented in the `mpmath` library [S4] with a test based on Sturm's theorem [S3], to ensure that all positive real roots are found. Those systems in which root finding fails—either because the Durand–Kerner algorithm fails to converge or because it finds an incorrect number of positive real roots—are discarded, but included in error estimates where reported.

C. Numerical samples

Table S1 gives the number of random Turing unstable systems from which distributions, averages, and probabilities were estimated for each $R \in \{2.5, 5, 7.5, 10, 12.5, 15, 17.5, 20\}$.

For $N = 3$, we ran both a search for general, non-binary systems and a (larger but numerically less expensive) search for binary systems only. Since the first search only yielded

TABLE S1. Number of random Turing unstable systems used to estimate distributions, averages, and probabilities for the different values of N, and corresponding figures.

N	Type	max T[a]	Reference[b]
$N = 2$	non-binary	10^7	Figs. 1, S1
$N = 3$	non-binary	10^4	
$N = 3$	binary	10^5	Figs. 2, 4, S1
$N = 4$	binary	10^5	Figs. 3, 4, S1
$N = 5$	binary	$2 \cdot 10^4$	Figs. 3, 4, S1
$N = 6$	binary	$2 \cdot 10^3$	Figs. 3, 4, S1

[a] Maximal number of Turing unstable systems.
[b] Figure (if any) in which results are shown.

binary global minima (as stated in our Letter), we used the results of the second, larger search for Figs. 3 and 4.

III. WAVENUMBER STATISTICS

In this Section, we discuss the wavenumber k_N^* at which a Turing instability first arises at $D_N = D_N^*$. In particular, as discussed in our Letter, we must ask whether a Turing instability is "observable at the system size". This observability requires the lengthscale $1/k_N^*$ of the linear instability to be (a) smaller than the system L and (b) larger than L/ℓ, for some scale difference $\ell > 1$. We are thus led to consider the probability $\mathbb{P}(K < k_N^* < \ell K)$, where $K = 1/L$.

It is instructive to start by considering the case $N = 2$. For the reaction-diffusion system in Eq. (1), a Turing instability arises for $D_2 = D_2^*$ at a wavenumber $k_2^* = (J/d_u d_v)^{1/4}$ [S1]. We stress that this value depends on d_u, d_v not only through their ratio $d = d_u/d_v$. To absorb the dependence on the dimensional system scale, it is natural to consider

$$\kappa_2(\ell) = \max_K \left\{\mathbb{P}\left(K < k_2^* < \ell K\right)\right\}, \tag{S20a}$$

as the maximal probability of a Turing instability being observable at some inverse system scale K over a fixed scale difference ℓ. We denote by $K_2(\ell)$ the corresponding maximizing inverse system size.

For $N > 2$, we correspondingly ask: what is the probability of a Turing instability being observable at this inverse system size? We therefore define

$$\kappa_N(\ell) = \mathbb{P}\left(K_2(\ell) < k_N^* < \ell K_2(\ell)\right) \quad \text{for } N > 2. \tag{S20b}$$

Figure S1 plots $\kappa_N(\ell)$ against N, for fixed values of R and ℓ, but the qualitative behaviour is independent of R and ℓ. We notice that $\kappa_N(\ell)$ increases slightly with N. If we restrict the analysis to those Turing unstable systems with $D_N^* \leqslant \mathcal{D}$, the probability is reduced somewhat for $N > 2$ compared to the case $N = 2$. This merely reflects the "fine-tuning problem": the wavenumber is strongly constrained for those very rare

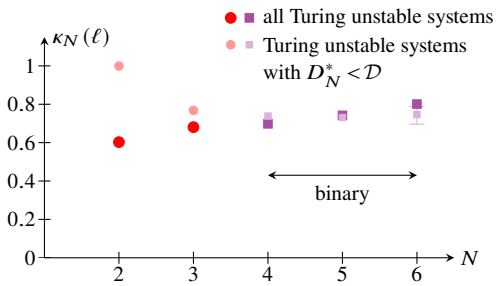

FIG. S1. Wavenumber statistics. Probability $\kappa_N(\ell)$ of a Turing instability being "observable" at a scale difference ℓ plotted against N; see text for further explanation. Larger markers: $\kappa_N(\ell)$ estimated from all Turing unstable systems; smaller markers: $\kappa_N(\ell)$ estimated from only those Turing unstable systems with $D_N^* < \mathcal{D}$. Parameter values: $R = 10$, $\ell = 10$, $\mathcal{D} = 5$. Asymmetric error bars again correspond to 95% confidence intervals larger than the plot markers, corrected for systems for which the numerics failed.

systems that have a "small" diffusive threshold at $N = 2$. Moreover, about three quarters of the Turing instabilities at $N > 2$ do arise at physical wavenumbers, so we can extend the observations in Figs. 2(d) and 3(c) to note that random kinetic Jacobians are still more likely to be unstable to an observable Turing instability with small diffusive threshold for $N > 2$ than for $N = 2$.

IV. DIFFUSION OF "SLOW" SPECIES

In the notation of Eq. (12) of our Letter, Ref. [S5] shows that Turing instability at $d = 0$ requires J_{22} to be stable (i.e. all its eigenvalues to have negative real part): if it is not, instabilities arise at arbitrarily small and therefore unphysical lengthscales. In particular, $\det \mathsf{J}_{22} \neq 0$, and so, using another result of Ref. [S5],

$$\det\left(\mathsf{J} - k^2\mathsf{D}\right) = \det \mathsf{J}_{22} \det\left(\mathsf{j} - k^2\mathsf{I}\right), \tag{S21}$$

where $\mathsf{j} = \mathsf{J}_{11} - \mathsf{J}_{12}\mathsf{J}_{22}^{-1}\mathsf{J}_{21}$. Hence a Turing instability occurs at $d = 0$ only if j has a positive real eigenvalue, as claimed in our Letter.

V. THE ASYMPTOTIC DIFFUSIVE THRESHOLD

Let $\mathsf{J} = O(1)$ be a Turing unstable kinetic Jacobian, with an eigenvalue λ destabilising at nearly equal diffusivities, so that $\mathsf{D} = \mathsf{I} + \mathsf{d}$ with $\mathsf{d} = o(1)$. The following claim extends an argument of Ref. [S6]:

Claim. J *has a defective zero eigenspace.*

Proof. Because $\mathsf{J} - k^2\mathsf{I}$ has a stable eigenvalue $\lambda - k^2$ and $-k^2\mathsf{d} \ll \mathsf{J} - k^2\mathsf{I}$, the corresponding eigenvalue of

$$\mathsf{J} - k^2\mathsf{D} = \left(\mathsf{J} - k^2\mathsf{I}\right) - k^2\mathsf{d}$$

can only have positive real part if $\lambda - k^2 = o(1)$ i.e. if $\lambda = o(1)$ and $k^2 = o(1)$ since $\mathrm{Re}(\lambda) < 0$. Hence J and $\mathsf{J} - k^2\mathsf{I}$ have a zero eigenvalue at leading order. Additionally, the eigenvalue correction from $-k^2\mathsf{d} = o\left(k^2\right)$ must be $O\left(k^2\right)$ at least, which occurs iff the (leading-order) zero eigenspaces of $\mathsf{J} - k^2\mathsf{I}$ and J are defective [S7]; this final implication is discussed in more detail in Ref. [S8]. □

The generic case is therefore $\mathsf{J} = \mathsf{J}_0 + O(\varepsilon)$, where $\varepsilon \ll 1$ and J_0 has a defective double zero eigenvalue.

Claim. $\mathsf{d} \gtrsim O\left(\sqrt{\varepsilon}\right)$*; in particular,* $\mathsf{D} - \mathsf{I} \gg \mathsf{J} - \mathsf{J}_0$.

Proof. Since J_0 has a defective double zero eigenvalue, J has two $O(\sqrt{\varepsilon})$ eigenvalues [S7], assumed to be stable (i.e. to have negative real parts). With $k = O(\varepsilon^\kappa)$, $\mathsf{d} = O\left(\varepsilon^\delta\right)$, destabilizing one of these requires, using the proof of the first claim above, $-k^2\mathsf{d} \gtrsim O(\varepsilon)$ and $-k^2\mathsf{I} \lesssim O(\sqrt{\varepsilon})$, i.e. $2\kappa + \delta \leqslant 1$ and $\kappa \geqslant 1/4$. Hence $\delta \leqslant 1/2$. This proves the claim. □

SUPPLEMENTAL CODE

The online Supplemental Material also includes excerpts from the `python3` code that we have written to implement the semianalytic approach for $N \geqslant 3$.

SUPPLEMENTAL REFERENCES

[S1] J. D. Murray, in *Mathematical Biology* (Springer, Berlin, Germany, 2002) Vol. II, Chap. 2, pp. 71–140, 3rd ed.

[S2] We were not able to compute this integral using MATHEMATICA. This is why, by contrast with the derivation of Eq. (S10), we have given the full details of the calculation above.

[S3] C.-K. Yap, in *Fundamental Problems in Algorithmic Algebra* (Oxford University Press, Oxford, England, 2000) Chap. 6 and Chap. 7, pp. 141–218.

[S4] F. Johansson, *`mpmath`: a `python` library for arbitrary-precision floating-point arithmetic* (version 1.1.0, 2018).

[S5] S. Smith and N. Dalchau, Model reduction enables Turing instability analysis of large reaction–diffusion models, J. R. Soc. Interface **15**, 20170805 (2018).

[S6] J. E. Pearson and W. Horsthemke, Turing instabilities with nearly equal diffusion coefficients, J. Chem. Phys. **90**, 1588 (1989).

[S7] E. J. Hinch, in *Perturbation Methods* (Cambridge University Press, Cambridge, UK, 1991) Chap. 1.6, pp. 15–18.

[S8] V. B. Lidskii, Perturbation theory of non-conjugate operators, USSR Comput. Math. Math. Phys. **6**, 73 (1966).